

THE EFFECT OF RAINFALL ON SLOPE STABILITY IN VIETNAM

TRINH MINH THU

Water Resources University, Hanoi, Vietnam

ABSTRACT: In recently years, number of slope failures with a large-scale have occurred in the mountainous areas and causing a big lost of human lives and properties. The slopes failures are usually occurred after heavy and long lasting rainfall. However, up to now the explanations of mechanism of the rainfall induced slope failures have not been extensively studied. In this paper the mechanism of the rainfall induced slope failures is studied. An example to calculate factor of safety for particular slope in the central Vietnam under rainfall conditions is presented. The results of this study serve as a foundation for explanation of the reduction of negative pore-water pressure, shear strength and then induced the slope failures. Meanwhile, the recover of negative pore-water pressure, shear strength and factor of safety of slope after rainfall stopped are discussed.

BACKGROUND OF THE RAINFALL INDUCED SLOPE FAILURES

Slope failures due to rainfall condition in Vietnam

Landslides are common occurrence in many parts of Vietnam. Number of slope failures with a large-scale have occurred in the mountain area and caused a lot of human lives and properties lost. The slopes failures are usually occurred after heavy and long duration of rainfall. Figure

1 show the landside occurred on the talus of the highway from Hoabinh to Sonla after heavy rainfall intensity. Especially, after heavily rainfall on 13/9/2009, a big landslide was occurred at Phinngan county, Batxat district, Laocai province and killed more than 20 people as shown in Figure 2. The landslides have not been occurred only on the steep slope along the highway but also occurred near the residential areas at the gentle slopes.



Figure 1 Landslide on the highway from Hoabinh to Sonla (Aug. 2005)



Figure 2 Landslide at Batxat – Laocai (on 27 Sep. 2005)

Mechanisms of the change in pore-water pressure in unsaturated soils

Some researchers have been investigated the effect of the rainfall on slope stability. However, there has been some debate as to the relative roles of antecedent and the

triggering rainfall. Experiences from different regions of the world have resulted in different conclusions as to the significance of antecedent rainfall for slope instability.

Figure 3 shows the pore-water pressure changes on unsaturated zone under static, evaporation and rainfall

conditions. The pore-water is normally negative under static equilibrium conditions with respect to the water table. The negative pore-water pressure head has a linear distribution with depth (line 1). Therefore, there can be no flow of water in the vertical condition. If the cover were removed from the ground surface, the soil surface would be exposed to the air. Therefore water in soils can flow out from the soil then would cause the pore-water pressure

to become more negative (e.g., pore-water pressure head line move to the left (line 2)). The maximum change in pore-water pressure will be at the near ground surface. The more evaporation time and greater intensity of the evaporation the more negative pore-water pressure will be. In other word, the pore-water pressure head line will be moved to the left.

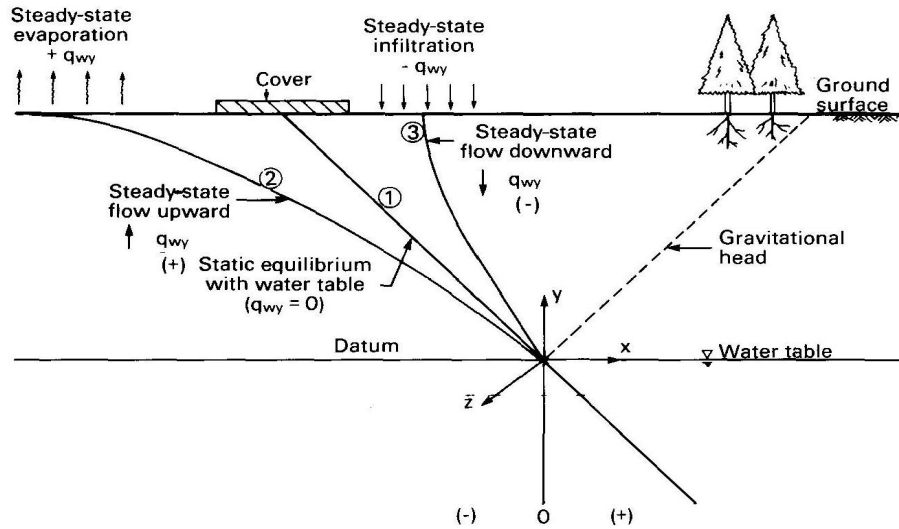


Figure 3 Cross-section of the pore-water pressure distribution in unsaturated zone (Fredlund and Rahardjo, 1993)

Steady-state infiltration causes a downward water flow. The negative pore-water pressure increases from the static equilibrium condition. Therefore, pore-water pressure head line will move to the right (line 3). The unsaturated zone will be getting smaller. As a result, the shear strength is decreased and then factor of safety decreased. The landslide is usually occurred on the residual soil layer in the mountain area. Therefore the volume and depth of the landslide is very much depended on the thickness of the residual soil and weathered rock layer.

Shear strength of unsaturated soil

Fredlund et al. (1978) proposed a shear strength equation using two stress state variables (i.e., net normal stress, $(\sigma - u_a)$ and matric suction, $(u_a - u_w)$) as follows:

$$\tau_{ff} = c' + (\sigma_{ff} - u_{af}) \tan \phi' + (u_a - u_w)_f \tan \phi^b \quad (1)$$

where:

- τ_{ff} shear stress on the failure plane at failure
- c' Intercept of the "extended" Mohr-Coulomb failure envelope on the shear stress axis when the net normal stress and the matric suction at failure are equal to zero. It is also referred to as the "effective

- cohesion"
- $(\sigma_{ff} - u_{af})$ net normal stress on the failure plane at failure
- σ_{ff} total normal stress on the failure plane at failure
- u_{af} pore-air pressure at failure
- ϕ' angle of internal friction associated with the net normal stress state variable, $(\sigma_{ff} - u_{af})$
- $(u_a - u_w)_f$ matric suction at failure
- u_{wf} pore-water pressure at failure
- ϕ^b angle indicating the rate of change in shear strength relative to changes in matric suction, $(u_a - u_w)_f$.

Equation (1) can be considered as an extension of the shear strength equation for a saturated soil. For an unsaturated soil u_w is smaller than u_a .

$$\tau_{ff} = C + (\sigma_f - u_a)_f \tan \phi' \quad (2)$$

Where: $C = c' + (u_a - u_w) \tan \phi^b$

At saturation u_w approaches u_a , causing matric suction to approach zero (i.e., $(u_a - u_w)$). At saturation condition

(i.e., $(u_a - u_w) = 0$) Equation (2) reduces to the familiar shear strength of a saturated soil as follows:

$$\tau_{ff} = c' + (\sigma_{ff} - u_{wf}) \tan \phi' \quad (3)$$

The Mohr-Coulomb envelope for saturated soils is commonly drawn as a two dimensional graph of shear stress versus effective normal stress (Figure 4). The failure envelope for unsaturated soils can be described in a three-dimensional plot. The three dimensional plot of failure

envelope for unsaturated soils is an extension of Figure 4 into the third dimension for the matric suction, $(u_a - u_w)$, axis which is illustrated in Figure 5. The angle relating the shear strength with respect to the matric suction (i.e., $(u_a - u_w)$) is characterized by ϕ^b . The angle of internal friction with respect to the net normal stress, $(\sigma - u_a)$, is defined by the angle ϕ' .

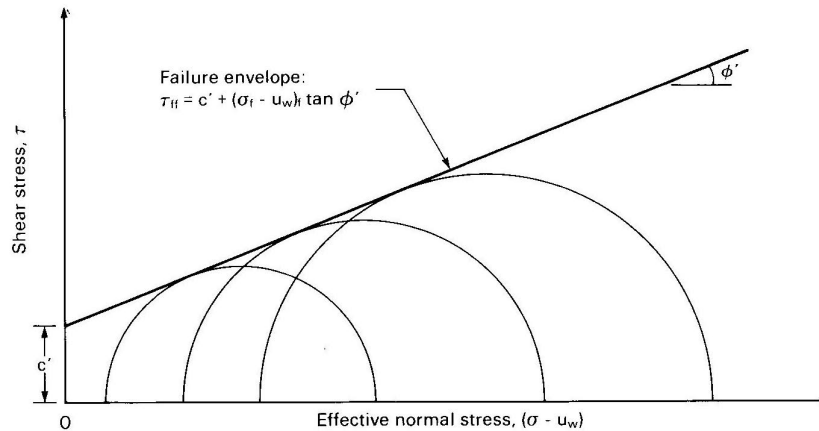


Figure 4 Mohr-Coulomb failure envelopes for saturated soils (after Fredlund and Rahardjo, 1993)

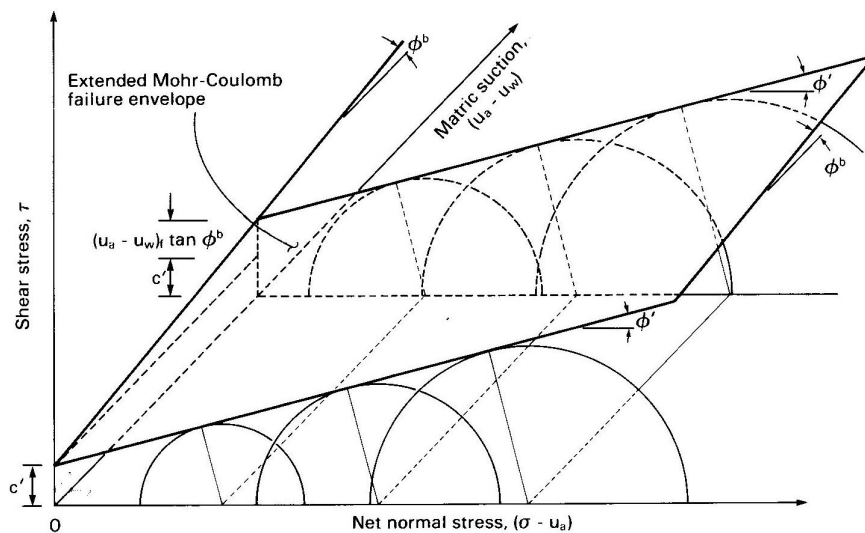


Figure 5 Extended Mohr-Coulomb failure envelopes for unsaturated soils (after Fredlund and Rahardjo, 1993)

PORE-WATER PRESSURE IN UNSATURATED ZONE DURING AND AFTER RAINFALL STOPS

In order to study the mechanism of the change in pore-water pressure in unsaturated soil (i.e., the zone above water table), the simulation of the unsaturated soil column was simulated. The soil column with 5m height and 0.5m in diameter was used in this study. Water table was

assumed to be at the bottom of the soil column. The coefficient of permeability of the soil is $k = 1 \times 10^{-6}$ m/s. Geo-studio 2004 software was used to simulate the rain water infiltration into the soil column with the flow rate of $q = 1 \times 10^{-5}$ cm/s.

Results and discussions

Figure 6 shows the change in pore-water pressure along the soil column with the time. The result from Figure 6 shows that the negative pore-water pressure goes to zero right after rainfall is occurred. The effect of the rainfall is decreased with depth. Negative pore-water pressure decreases during rain water infiltration into soil column as a result the shear strength decrease. However, Figure 6 also shows that there is not completely saturated in soil column.

In order to study the distribution of pore-water after rain stops, the model of the soil column during drying process

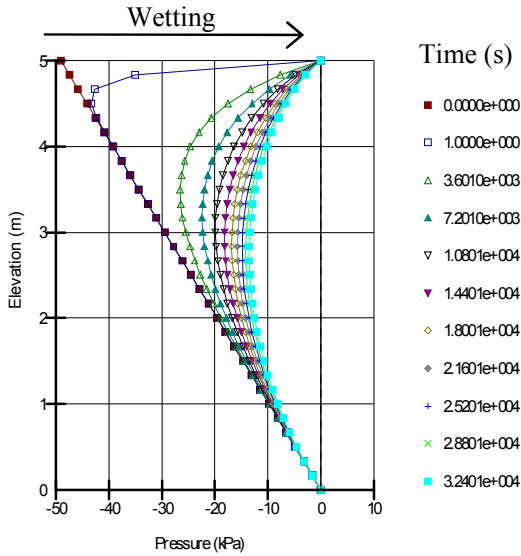


Figure 6 Distribution of pore-water pressure with time along the soil column during wetting stage

was simulated. The boundaries condition of this problem were the same with the boundaries condition for the rain water infiltration simulation accept no water flow was applied on the ground surface of the soil column. Figure 7 shows the pore-water pressure distribution along the soil column with time during drying stage. The result from Figure 7 shows that the pore-water pressure became negative quickly at near the ground surface. During drying stage, the negative pore-water pressure increase and then increase in shear strength as a result the factor of safety increase. However, negative pore-water pressure recovers very slowly at this stage.

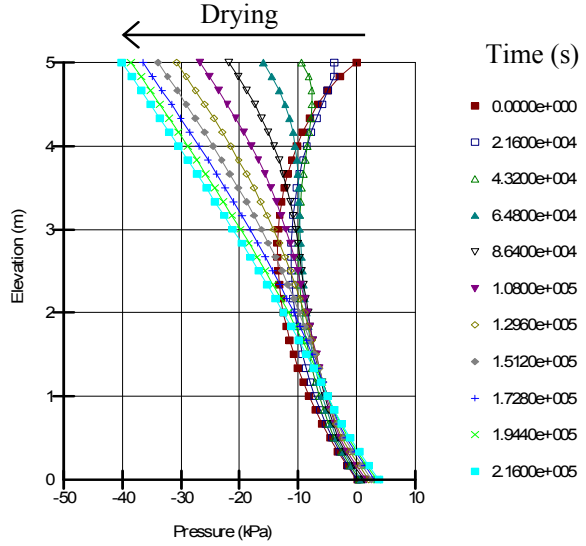


Figure 7 Distribution of pore-water pressure with time along the soil column during drying stage

THE EFFECT OF THE RAINFALL ON SLOPE STABILITY

In order to study the effect of the rainfall on slope stability, the slope on talus of the highway at Tamky-Tienphuoc (at 23km south of Tamky town) was chosen for slope stability calculation. The residual soil is silty clay with gravel of the thickness of 7m. The soil properties

used in the slope stability calculation as shown in table 1. The angle ϕ^b (angle indicating the rate of change in shear strength relative to changes in matric suction, $(u_a - u_w)_f$) was assumed to be 1/2 of the value ϕ' , The water table was assume at 44m below ground surface.

Table 1 Soil properties have been used in the simulation

| TT | Coefficient of permeability, k (m/s) | Density γ_{tm} (kN/m ³) | Friction angle, ϕ' (degree) | Effective cohesion, c' (kPa) | ϕ^b (degree) |
|----|--|--|----------------------------------|--------------------------------|-------------------|
| 1 | 1×10^{-6} | 18,5 | 13 | 10 | 6 |
| 2 | 5×10^{-6} | 19,5 | 20 | 10 | 10 |

Simulation of the seepage during and after rainfall stops

The pore-water pressures, u_w , during rainfall are obtained from the seepage analysis using SEEP/W (Geo-studio,

2004). Figure 8 shows the geometry and mesh of the example utilized for the steady and transient seepage analyses. In the transient seepage analysis, boundary flux, q , equal to 1.0×10^{-5} cm/s is applied to the surface of the soil slope. Evaporation and evapotranspiration are not simulated in this study. The applied boundary flux, q is reviewed by elevation in order to avoid ponding. The net

flux, Q , is taken to be zero along the sides of the slope above the groundwater table and along the bottom line. The total head boundary is applied along the sides of the slope below the groundwater table. The finite elements mesh and boundaries condition is shown in Figure 8.

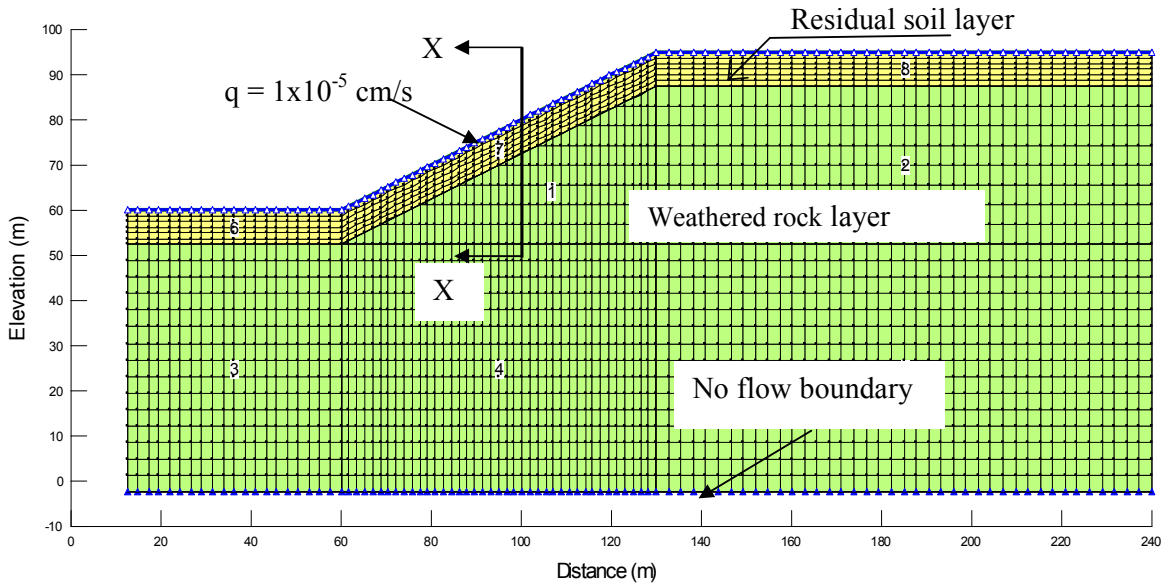


Figure 8 Geometry and finite element mesh for seepage analysis

A rainfall of 1.0×10^{-5} cm/s falls on the slope for 6 hours. The seepage analyses of rain water infiltration into the slope can be performed using the following governing equation:

$$\frac{\partial}{\partial x} \left(k_w \frac{\partial h_w}{\partial x} \right) + \frac{\partial}{\partial y} \left(k_w \frac{\partial h_w}{\partial y} \right) = m_2^w \rho_w g \frac{\partial h_w}{\partial t} \quad (4)$$

where:

k_w = water coefficient of permeability,

$\frac{\partial h_w}{\partial x}$ = hydraulic gradient in the x direction,

$\frac{\partial h_w}{\partial y}$ = hydraulic gradient in the y direction,

$\frac{\partial h_w}{\partial t}$ = change in hydraulic head with time,

m_2^w = coefficient of water volume change with respect to change in matric suction

ρ_w = density of water, and

g = acceleration due to gravity

Result and discussion

Figure 9a shows the pore-water pressure, u_w , profiles at Section X-X (i.e., at the middle of the slope) during 6 hours of rainfall. The pore-water pressure, u_w , increases with time in the unsaturated zone. The groundwater table appears to remain at the same elevation during the rainfall period, indicating that the percolation of rain water has not reached the groundwater table. Figure 9b shows the pore-water pressure, u_w , profiles at Section X-X during drying process. The negative pore-water pressures are recovered during the drying process. It should also be noted that the groundwater table rises during the drying stage due to the percolation of rainwater that has reached the groundwater table at this stage.

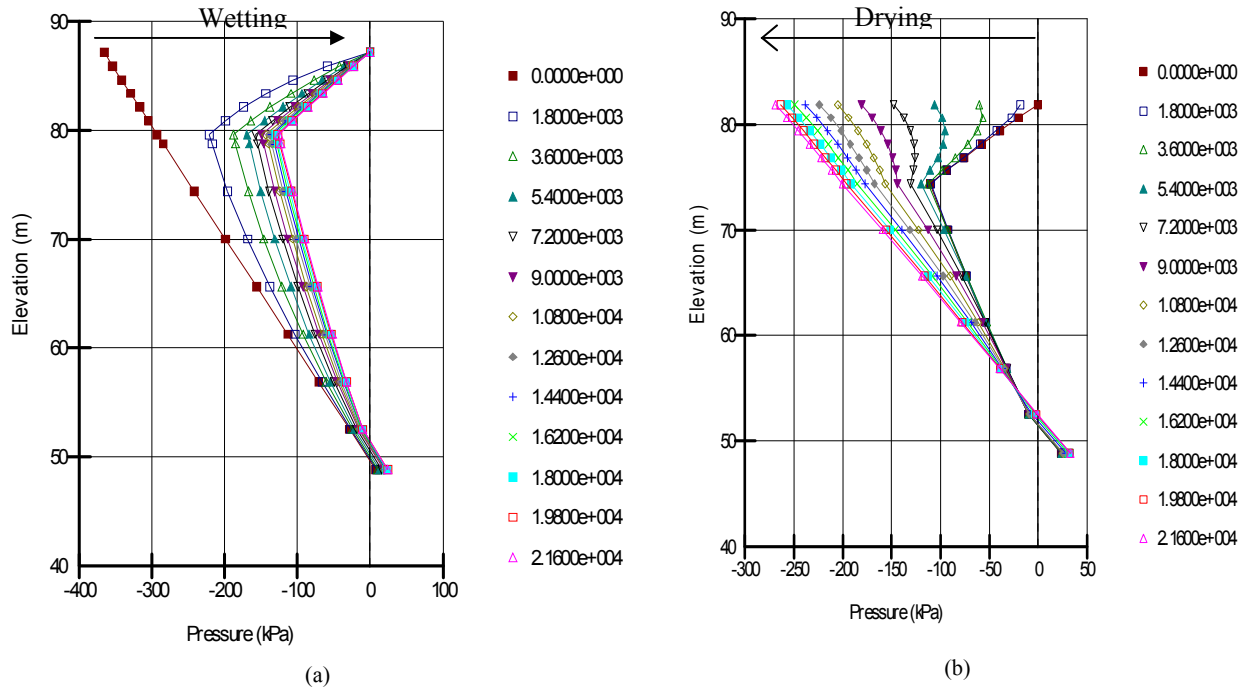


Figure 9 Pore-water pressure profiles at Section X-X; (a) During infiltration; (b) during drying process

Slope stability analysis

The pore-water pressures calculated from the transient seepage analyses are exported to SLOPE/W (Geo-studio, 2004) for the analyses of slope stability at different times

during the rainfall and drying periods. The general equation to calculate the factor of safety, F_s , based on Bishop's Simplified method is as follows (Fredlund and Rahardjo, 1993):

$$F_s = \frac{\sum \left[c' \beta R + \left\{ N - u_w \beta \frac{\tan \phi^b}{\tan \phi'} - u_a \beta \left(1 - \frac{\tan \phi^b}{\tan \phi'} \right) \right\} R \tan \phi' \right]}{A a + \sum W x - \sum N f} \quad (5)$$

where:

- F_s = factor of safety with respect to moment equilibrium,
- c' = effective cohesion,
- β = sloping distance across the base of a slice,
- R = the radius for a circular slip surface or the moment arm associated with mobilized shear force, S_m , for any shape of slip surface.
- N = the total normal force on the base of the slice,
- ϕ' = effective angle of internal friction,
- ϕ^b = angle indicating the rate of increase in shear strength relative to the matric suction,
- u_w = pore-water pressure,
- u_a = pore-air pressure,
- A = the resultant of external water force,
- a = the perpendicular distance from resultant of external water force to the centre of rotation or to the centre of moments,
- W = the total weight of the slice of with 'b' and height 'h', and
- f = the perpendicular offset of the normal force from the centre of rotation or from the centre of moment.

The soil properties utilized in the slope stability analyses are presented in Table 1. The soil parameters used are representative values for the Tamky-Tienphuoc residual soil.

Figure 10 shows the factor of safety obtained from slope stability analysis with time during infiltration and drying processes. The factor of safety was 1.502 (Table 2) before

rainfall and decreased as rain water infiltrated into the slope. After 6 hours of rainfall the factor of safety was 0.977, indicating that failure could have occurred. Subsequently the factor of safety increased gradually after the rainfall had stopped. The factor of safety was 1.293 at 6 hours after the rain had stopped.

Table 2 Factor of safety during and after rainfall stops

| During rainfall | | | | | | | | | | | | | |
|----------------------|-------|-------|-------|-------|-------|-------|-------|-------|-------|-------|-------|-------|-------|
| Time (h) | 0,0 | 0,5 | 1,0 | 1,5 | 2,0 | 2,5 | 3,0 | 3,5 | 4,0 | 4,5 | 5,0 | 5,5 | 6,0 |
| Fs | 1,502 | 1,166 | 1,092 | 1,056 | 1,034 | 1,019 | 1,009 | 1,000 | 0,994 | 0,989 | 0,984 | 0,981 | 0,977 |
| After rainfall stops | | | | | | | | | | | | | |
| Time (h) | 0,0 | 0,5 | 1,0 | 1,5 | 2,0 | 2,5 | 3,0 | 3,5 | 4,0 | 4,5 | 5,0 | 5,5 | 6,0 |
| Fs | 0,984 | 0,989 | 1,012 | 1,040 | 1,075 | 1,111 | 1,146 | 1,180 | 1,211 | 1,237 | 1,260 | 1,279 | 1,293 |

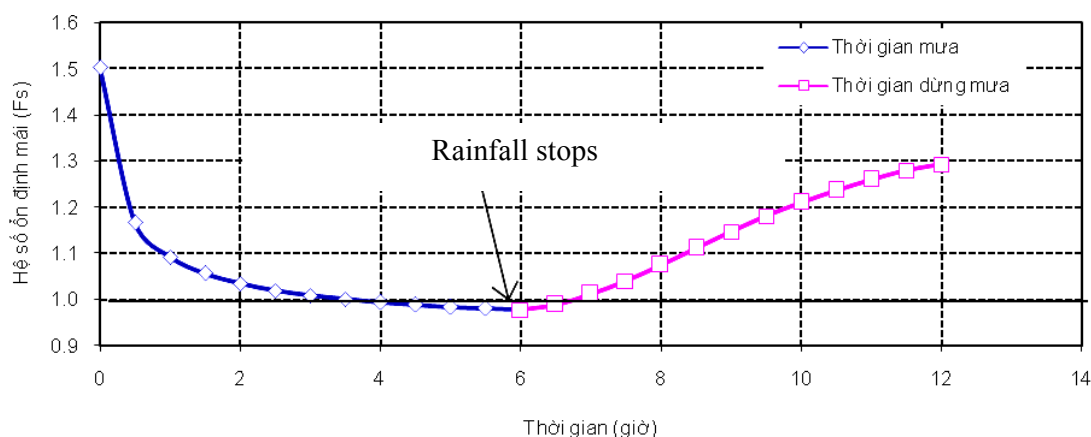


Figure 10 Factor of safety versus elapsed time during infiltration and drying processes.

SUMMARY AND RECOMMENDATIONS

The results from this study can be drawn as some remarks and conclusions as follow:

- The antecedent rainfall prior to the storm events has decreased the matric suction in the slope causing the coefficient of permeability of the soil to increase, making the soil more permeable to infiltration. As a result, the shear strength decreases and consequently, the factor of safety of the slope decreases during rainfall.
- The quantity of the change in pore-water pressure, matric suction, shear strength and factor of safety of the slope during rainfall and during drying stage were investigated.
- The couple between SEEP/W and SLOPE/W for simulation of change in factor of safety during rainfall

and during drying stage was studied. The results of this study provided the general picture of relationship between factor of safety and the rainfall duration as well as during drying stage.

- The results from this study can be provided the basis explanation of the landslide due to rainfall. Also it can be used as a procedure for design, construction for prevention and mitigation of the landslide due to rainfall.

REFERENCES

- Fredlund D.G. and Karhn J. (1977), Comparison of stability methods of analysis. *Canadian geotechnical journal*, Vol. 14, No.3, pp.429-439.
- Fredlund DG và Rahardjo H (1998), *Unsaturated Soil Mechanics*, (Sách dịch Cơ học đất không bão hòa,

- Nhà xuất bản Giáo dục, Người dịch: NC Mẫn, N Uyên, NT Tiến, TM Thu)
- Fredlund D.G. (1997), The analysis of slope – *Short course* document in Water Resource University
- Nguyen Cong Man, Trinh Minh Thu and Nguyen Cong Thang. Fundamentant of Unsaturated Soil and Geo-Slope Office. Lectures for Geotechnical Engineering Master
- H. Rahardjo, EC. Leong và Trịnh Minh Thu (2005) "Application of soil-Water characteristic curve in geotechnical engineering". *Proceedings of the international workshop, Hanoi geoengineering 2005*, p.86 - 94.
- Trinh Minh Thu, (1999). History of Slope Stability Researches in the World" Pro. Vietnam Geological and Geoenvironmental Engineering.
- Trinh Minh Thu, Rahardjo and Leong (2006) "Shear strength and pore-water pressure characteristics during constant water content triaxial tests". *Journal of Geotechnical and geoenvironmental engineering*, American Society of Civil Engineering, p.411- 419.
- Trịnh Minh Thu, H. Rahardjo and EC. Leong (2006) "Effects of Hysteresis on Shear Strength Envelopes from Constant Water Content and Consolidated Drained Triaxial Tests". *Proceedings of the International conference on Unsaturated soils*, Arizona, USA.
- Trinh Minh Thu, Nguyen Uyen, (2010). Prevention Rock Failure in Slope. Publishing of Building.
- Whitlow, R. (1996), Soil Mechanics, "Cơ học đất tập 1 và 2 - Bản dịch", NXB Giáo dục Hà Nội.